Eur. Phys. J. Spec. Top. (2026) 235:8675–8690
https://doi.org/10.1140/epjs/s11734-026-02477-7

THE EUROPEAN PHYSICAL JOURNAL SPECIAL TOPICS

Regular Article

Functional network analysis of macroeconomic indicators: synchronization dynamics and systemic risk

Semen Kurkin[1,a], Vladimir Khorev[1,b], Alexander Shenderyuk-Zhidkov[2,c], and Alexander Hramov[1,d]

[1] Plekhanov Russian University of Economics, 36, Stremyanny per., Moscow 115054, Russia
[2] Independent Researcher, Kaliningrad, Russian Federation

Received 25 May 2026 / Accepted 19 June 2026 / Published online 8 July 2026
© The Author(s), under exclusive licence to EDP Sciences, Springer-Verlag GmbH Germany, part of Springer Nature 2026

Abstract This study applies functional network analysis to investigate the synchronization dynamics of the Russian economy. Understanding how macroeconomic indicators co-move over time is crucial for identifying systemic vulnerabilities, crisis propagation mechanisms, and sectoral integration patterns. Our main methods include constructing functional networks from 72 monthly time series of Russian macroeconomic indicators (February 2008–February 2025). Nodes represent individual indicators. Edges denote statistically significant correlations between indicator time series within moving time windows. We compute standard network metrics: node degree, node strength (weighted degree), clustering coefficient, modularity, average path length, network density, and node centrality measures. Our analysis reveals that during crisis periods, average node degree and network density increase sharply, indicating widespread synchronization across sectors. Node strength proves more sensitive than degree to systemic shocks. Modularity decreases during crises, reflecting breakdown of sectoral independence. Average path length shortens, implying faster shock transmission. Clustering coefficients rise, forming "monolithic" blocks of tightly co-moving indicators. Centrality measures identify the ruble exchange rate, industrial production, and the Bank of Russia key rate as systemically important transmission nodes. Functional network analysis provides a quantitative framework for monitoring macroeconomic systemic risk. Rising average degree and density, coupled with falling modularity and path length, serve as early warning signals of crisis propagation. The approach helps identify which indicators become "systemic hubs" under stress, offering potential guidance for policy interventions and macroprudential surveillance. The rising local clustering coefficient, which counts closed triangles around each indicator, can be interpreted as the simplest higher-order (triadic) interaction signature of the system; together with the breakdown of modularity it describes the self-organization of macroeconomic indicators into a globally synchronized regime under stress. Pearson- and Spearman-based networks yield qualitatively identical dynamics throughout the sample, providing an internal robustness check.

Abbreviations

AI	Artificial intelligence
CGE	Computable general equilibrium
DSGE	Dynamic stochastic general equilibrium
FNAR	Functional network autoregressive model
GDP	Gross domestic product
ITN	International trade network
VAR	Vector autoregression

[a] e-mail: kurkinsa@gmail.com (corresponding author)
[b] e-mail: khorevvs@gmail.com
[c] e-mail: a.shenderyuk@yandex.ru
[d] e-mail: hramov.ae@rea.ru

1 Introduction

A persistent challenge in macroeconomic analysis is the limitation of traditional methodologies that prioritize the study of individual indicators or isolated pairwise relationships. Historically, the field has relied on aggregate metrics, such as gross domestic product (GDP), inflation rates, and unemployment figures, operating under the assumption that these discrete data points, when observed concurrently, provide a sufficient approximation of economic health. However, as global markets have become increasingly interconnected and complex, this approach has shown a significant failure to capture the emergent systemic effects that arise when multiple parameters shift simultaneously. Traditional models, including many computable general equilibrium (CGE) and vector autoregressive (VAR) frameworks, often assume a static or neutral institutional backdrop, treating the economy as a system that fluctuates around a stable equilibrium. This perspective frequently overlooks the reality that the very architecture of economic relationships transforms during periods of turbulence, leading to non-linear shifts and structural dislocations that aggregate indicators cannot predict [1, 2].

The conceptual gap in conventional analysis is most evident during extreme crises, such as the 2008 financial collapse or the COVID-19 pandemic. During such episodes, the economy does not merely experience a shift in values; it undergoes a fundamental reconfiguration of its internal connectivity [3]. Traditional methods struggle with "granular financial dislocation," where micro-level failures—such as the collapse of a specific interbank lending channel or a disruption in a specialized supply chain—propagate through the system via mechanisms of contagion and amplification. These systemic risks are often endogenous, arising from the collective behavior of economic agents whose individual choices may appear rational but whose aggregate impact creates instability [2]. To address these shortcomings, the approach proposed here, based on the theory of functional networks of macroeconomic indicators, shifts the focus from the magnitude of variables to the topology of their interactions [4].

The limitation of studying indicators in isolation is further compounded by the "mechanisms, not metaphors" principle. Policymakers often rely on historical analogies (e.g., comparing current inflation to the 1970s), which can be analytically dangerous, because the underlying global linkages and institutional structures have evolved. Functional network theory moves beyond these analogies by identifying recurring mechanisms—such as credit booms, supply shocks, and the interaction of trade conflicts with expectations—that operate through specific network topologies. This allows for a more nuanced understanding of how a given shock will have different effects in different institutional environments based on the density, efficiency, and modularity of the economic network [1, 4].

Functional connectivity is typically established through correlation or causality tests, mapping how the dynamics of one indicator propagate to others [5]. For instance, in a multivariate time series, directed edges may capture dynamic Granger-causal relations (where past values of one series help predict future values of another), while undirected edges encode contemporaneous conditional dependencies [6]. This approach is closely related to VAR models but extends them by focusing on the sparsity and architecture of the coefficient matrices, allowing for the identification of functional hubs—indicators that exert a disproportionate influence on the rest of the system [4].

The structural properties of these networks, such as centrality, hub detection, and modularity, provide profound insights into the roles of specific indicators. Centrality measures—including degree, betweenness, and closeness—quantify a node's capacity to influence or be influenced by the rest of the network. In a modular network, centrality measures that quantify local neighborhood influence can be dissociated from those that index global influence, allowing analysts to identify sectors that may be local leaders but not global systemic threats. This distinction is critical for macroprudential policy, as it enables the targeting of specific nodes responsible for global systemic stability [7].

The principle of complementarity explains how the architecture of economic relationships is built on specialized "functional modules"—groups of nodes performing similar tasks that are key to structural changes in the economy. Over extended periods, the configuration of these modules dictates national growth trajectories. Unlike social networks, where information might spread through "weak links," functional networks rely on the precise matching of customer needs with supplier capabilities [8]. This matching can be modeled using the "matching-centrality" framework, which decomposes the linking probability between two nodes into an assortative matching term (who makes links with whom) and a centrality term (how many links are made). This decomposition provides a precise fit for observed economic networks, enabling the prediction of missing links and the identification of latent traits that drive node behavior [9].

The relevance of these motifs extends to international trade. The International Trade Network (ITN) demonstrates scale-free and small-world properties, where a few highly connected countries act as hubs for global commerce [10]. This hierarchy implies the system is robust to random failures but vulnerable to targeted disruptions of the core [11]. Applying a functional lens to trade data reveals that "proportional traders"—countries that engage with high-GDP, resilient partners—experience lower "avalanche sizes" (the systemic impact of their collapse) compared to those that concentrate trade on low capacity, vulnerable partners. This suggests that the architecture of a country's trade relationships is a better predictor of its systemic risk than its individual GDP [12].

Table 1 Comparison of the forecasting and analysis models

Characteristics	VAR models	DSGE models	Functional networks
Model type	Non-structural, econometric	Structural, theoretical	Topological, data-driven
Primary purpose	Forecasting indicators	Policy analysis, scenarios	Analysis of structure and systemic risks
Number of variables	Limited (5–15)	Limited by structure	Scalable (100+)
Analysis of structural dynamics	Not provided	Not provided	Central focus

Connectivity also plays a dual role in financial resilience. On one hand, a more dense and symmetric configuration can provide resilience by allowing shocks to be absorbed and diluted across many nodes. On the other hand, past a certain threshold of interconnectedness, the likelihood of a systemic collapse can actually increase, as the system becomes too tightly coupled to isolate a crisis. This nonlinear relationship between density and stability necessitates the use of advanced models, such as functional network autoregressive (FNAR) models, to monitor the shifting dynamics of risk transmission in real time [2, 13].

According to the literature, three main classes of models for forecasting and policy analysis are distinguished: large-scale macroeconometric models, VAR models, and DSGE models [14, 15]. Our approach occupies a unique niche, intersecting with each of these categories without fitting neatly into any single one (Table 1).

The framework we develop also connects to two themes central to the present special issue: *self-organization* and *higher-order interactions* in complex networks. Stress-induced synchronization across macroeconomic sectors—the disappearance of modular boundaries and the formation of densely co-moving blocks—is naturally cast in the language of collective self-organization, in which the system spontaneously reorganizes into a low-dimensional, globally coherent state without external coordination. In parallel, the local clustering coefficient, which counts closed triangles around each node, is the simplest indicator of higher-order interaction: it directly measures the density of 2-simplices in the functional graph and complements purely pairwise (dyadic) descriptors, such as degree and node strength. We, therefore, treat the joint dynamics of modularity, density, and clustering as a low-dimensional fingerprint of self-organized, higher-order reconfiguration of the macroeconomic system during crises.

2 Materials and methods

Our methodology synthesizes modern complex network theory with classical econometric analysis. Functional networks of macroeconomic indicators conceptualize the economy not as a set of isolated variables, but as a living ecosystem of interconnected processes, where each indicator is a node and the correlations between them form the edges of the graph (see examples in Fig. 2 and the overall analytical pipeline in Fig. 1).

The analytical pipeline (Fig. 1) proceeds in four logical steps. (i) A panel of 72 monthly macroeconomic time series spanning six sectors (commodity, exchange, financial, real, monetary, external) is treated as a functional network whose nodes are individual indicators. (ii) For each rolling window we compute pairwise Pearson and Spearman correlations and threshold them by statistical significance, producing a sequence of weighted undirected graphs $G_{T_1}, \ldots, G_{T_N}$ with edge weights $w_{ij} = |\rho_{ij}|$. (iii) Node-level topological metrics—strength s_i, clustering coefficient C_i, degree and betweenness centrality—characterise the systemic role of each indicator and, in the case of C_i, provide a direct measure of higher-order (triadic) interaction. (iv) Global network-averaged metrics (density, modularity, average path length, average clustering, eigenvector centrality, efficiency) are computed over the annual sliding window to track aggregate dynamics and crisis-driven self-organization.

2.1 Data description

The empirical analysis utilizes a panel of $N = 72$ monthly macroeconomic time series for the Russian Federation (a full list is provided in the Appendix), covering the period from February 2008 to February 2025. The dataset encompasses all principal segments of the economic system:

- Commodity markets: Prices of Brent, Dubai, WTI, and Urals crude oil, and gold.

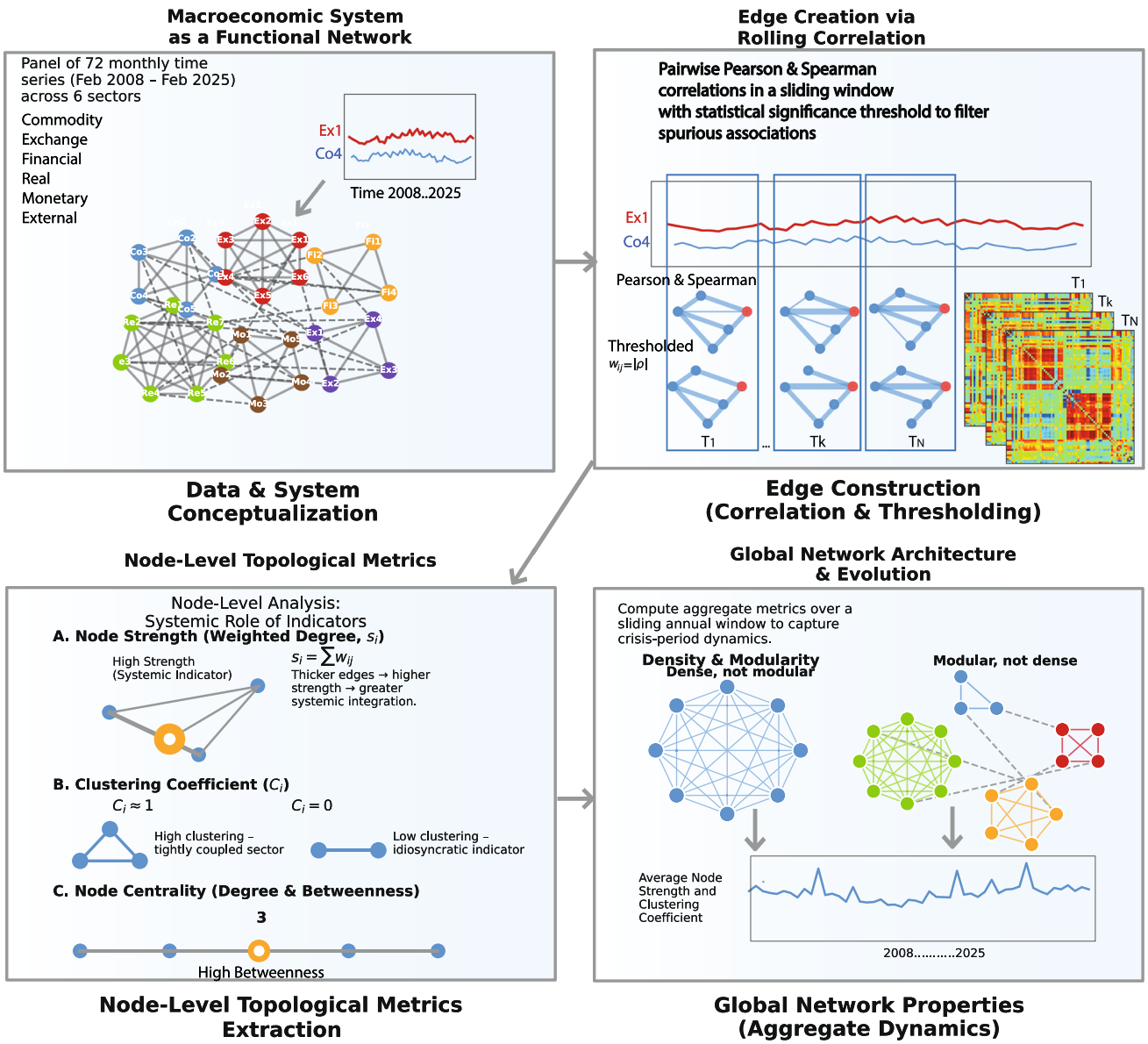


Fig. 1 Schematic overview of the analytical pipeline. Top-left: data and system conceptualization—72 monthly indicators (Feb 2008–Feb 2025) across six sectors are mapped to nodes of a functional network. Top-right: edge construction via rolling Pearson and Spearman correlations followed by a statistical-significance threshold, yielding a sequence of weighted graphs $G_{T_1}, \ldots, G_{T_N}$ with $w_{ij} = |\rho_{ij}|$. Bottom-left: node-level metrics characterising the systemic role of each indicator (node strength, clustering coefficient, degree and betweenness centrality). Bottom-right: global network architecture and its evolution—density, modularity, and aggregate dynamics over the rolling window capturing crisis-period behaviour

- Exchange rates: USD/RUB, EUR/USD, real effective exchange rate of the ruble, and USD indices against developed-market currencies.
- Financial markets: RTS and Moscow Exchange indices, Dow Jones, S&P 500, Nasdaq, and yields on Russian and US sovereign bonds across multiple maturities.
- Real sector: GDP variants, industrial production indices, and sectoral output data for mining, manufacturing, construction, freight turnover, retail and wholesale trade, paid services, and catering. Selected indicators are represented as year-on-year growth rates, seasonally adjusted indices, or absolute indexed values.
- Monetary block: M2 and M2X aggregates, and the Bank of Russia key policy rate.
- External sector: Current account balance, trade balance, goods and services exports/imports, capital flows, and international reserves.

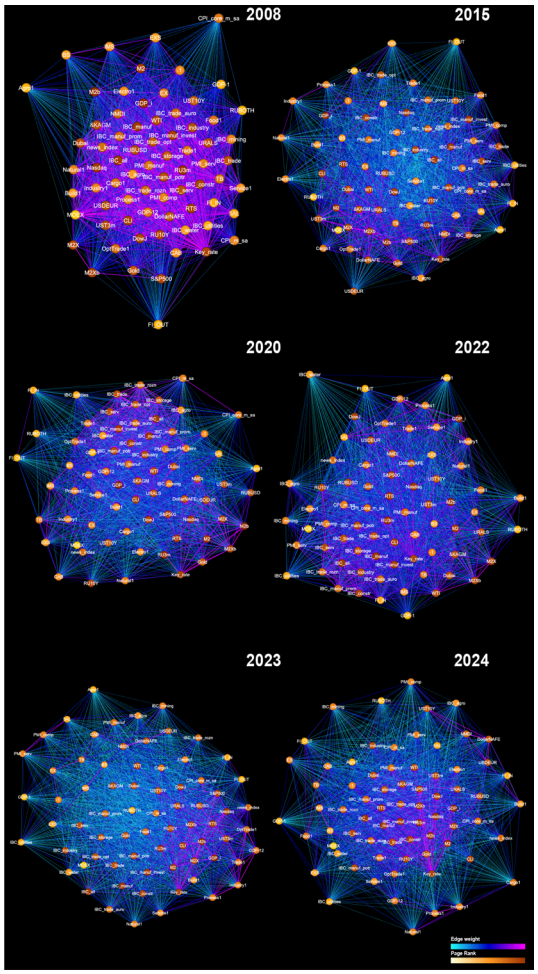


Fig. 2 Functional networks of macroeconomic indicators for 2008, 2015, 2020, 2022–2024. Shown here for qualitative illustration of the resulting graph structure and its inter-annual variability; all quantitative results in this paper are based on the rolling-window network metrics reported in Figs. 3, 4, 5, 6

The dataset includes 24 business climate indicators from the Bank of Russia's enterprise survey (IBC series). These indicators are disaggregated by sector (industry, manufacturing, construction, trade, services, agriculture, etc.) and by sub-sector. While this granularity provides valuable sectoral detail, readers should note that the IBC block is over-represented relative to other economic domains. Consequently, within-IBC correlations may contribute disproportionately to global network metrics, such as average degree and density.

2.2 Functional network construction

Let the set of $N = 72$ macroeconomic indicators be denoted by $\mathcal{V} = \{v_1, \ldots, v_N\}$. For each indicator v_i we have a time series $\{x_i(t)\}_{t=1}^{T}$ with sample rate equal to month, where T spans February 2008 to February 2025.

We consider a sliding time window of fixed length $W = 12$ months. For each starting month $\tau = 1, 2, \ldots, T - W + 1$, the data segment $\{x_i(t)\}_{t=\tau}^{\tau+W-1}$ is used to construct a functional network $G_\tau = (V, E_\tau)$. The node set $V = \mathcal{V}$ remains identical for all τ; only the edge set E_τ and the associated weights evolve with τ.

The input time series comprise a mixture of stationary series (year-on-year growth rates, interest rates, survey diffusion indices) and non-stationary series (e.g., M2). Within each 12-month rolling window, all series are treated as given without differencing or detrending. This approach is justified on three grounds: (i) the 12-month window length is sufficiently short that deterministic trends within the window are minimal for most level series; (ii) Spearman correlation, employed alongside Pearson, is robust to monotonic trends and non-normality; (iii) our primary interest lies in the change in correlation structure across windows. This is a differencing operation that removes common trends would also eliminate the very co-movement patterns we seek to measure [16].

For a given window τ, we compute the pairwise correlation between every pair of indicators (v_i, v_j). Both Pearson's correlation coefficient $r_{ij}(\tau)$ and Spearman's rank correlation coefficient $\rho_{ij}(\tau)$ are calculated in parallel. The absolute value $|r_{ij}(\tau)|$ (resp. $|\rho_{ij}(\tau)|$) is taken as a measure of co-movement strength. An undirected edge $e_{ij} \in E_\tau$ is established between nodes v_i and v_j if the corresponding correlation is statistically significant at the level $p < 0.05$. Significance is assessed using a two-sided test with the null hypothesis of no correlation; for Pearson,

a Student's t test is employed, while for Spearman, an exact permutation or asymptotic t-approximation is used. No adjustment for multiple comparisons was applied at the edge-selection stage. This choice follows standard practice in the functional network literature for macroeconomic applications, where the goal is to preserve the full correlation structure rather than enforce strict type I error control that would eliminate a substantial portion of meaningful economic relationships [17, 18]. A sensitivity analysis using FDR-corrected thresholds ($q = 0.05$) confirms that while edge counts decrease by approximately 30%, the temporal dynamics of global network metrics remain qualitatively unchanged.

Edges that pass the significance threshold are assigned a weight:

$$w_{ij}(\tau) = |r_{ij}(\tau)| \quad (\text{or } |\rho_{ij}(\tau)|) \tag{1}$$

and are stored in the weighted adjacency matrix $\mathbf{W}_\tau$. Consequently, each τ yields a weighted undirected graph $G_\tau = (V, E_\tau, \mathbf{W}_\tau)$.

The absolute value transformation $w_{ij} = |\rho_{ij}|$ is adopted, because standard graph-theoretic metrics employed in this study, including clustering coefficient, modularity, and average path length, are defined for non-negative edge weights. Treating negative correlations as positive edges of equal magnitude preserves the strength of co-movement while acknowledging that the economic interpretation of sign differs across indicator pairs. To address the potential loss of sign information, The fraction of negative edges per rolling window, on average is 0.322, with negative edges most prevalent during crisis periods.

The sliding window is advanced by 1 month at a time, producing a sequence of graphs:

$$\{G_\tau\}_{\tau=1}^{T-W+1} \tag{2}$$

which captures the temporal evolution of the macroeconomic functional connectivity. The window length $W = 12$ months guarantees a sufficient number of observations for stable correlation estimates while preserving the ability to track annual dynamics. All global and local network metrics reported in this paper are computed on each G_τ and then analysed over τ.

Two correlation measures (Pearson and Spearman) are processed independently throughout the entire sequence. The resulting network dynamics are qualitatively identical for both measures (see Sect. 3.2), and their close agreement serves as an internal robustness check against the choice of linear vs. monotonic dependence. The sequence $\{G_\tau\}$ forms the basis for the topological analysis presented in the following sections.

2.3 Topological metrics and analytical framework

To quantify the structural properties and temporal evolution of the network, the following graph-theoretic measures are computed:

2.3.1 Node degree (k_i)

The degree of node i denotes the number of statistically significant connections incident to the indicator. Economically, a high degree reflects broad co-movement with other macroeconomic variables, signaling systemic rather than idiosyncratic behavior. Aggregate increases in average degree are typically associated with periods of heightened macroeconomic synchronization, such as systemic stress episodes [19].

2.3.2 Weighted degree (node strength, s_i)

Defined as $s_i = \sum_j w_{ij}$, node strength incorporates both the quantity and intensity of an indicator's connections. Strength is particularly sensitive to structural shifts in correlation magnitudes and serves as a proxy for the robustness of an indicator's integration into the broader macroeconomic system [20].

2.3.3 Clustering coefficient (C_i)

The local clustering coefficient measures the probability that neighbors of node i are also mutually connected. High clustering indicates the presence of tightly coupled indicator groups, which can be interpreted as coherent economic sectors or functional blocks. Sustained increases in clustering during downturns reflect the formation of rigid, highly synchronized macroeconomic regimes [21, 22]. From a higher-order interactions perspective, C_i counts the density of closed triangles around node i and is, therefore, the simplest measure of triadic (2-simplex) interaction in the functional graph. It captures coordinated co-movement of indicator triples that cannot be reduced

to the underlying pairwise (dyadic) connections alone, and provides the most direct entry point for a higher-order reading of synchronization dynamics in the macroeconomic network.

2.3.4 Modularity (Q)

Modularity quantifies the extent to which the network partitions into densely connected communities with sparse inter-community links. High modularity implies structural segmentation into relatively autonomous economic subsystems (real vs. financial sectors), whereas declining modularity indicates increasing cross-sectoral integration or systemic convergence [23, 24].

2.3.5 Average path length (L)

Average path length is the mean shortest path distance between all node pairs in the network. Shorter path lengths imply rapid propagation of shocks across the system. A contraction in L typically accompanies crisis periods, reflecting accelerated transmission of macroeconomic disturbances through newly formed or strengthened linkages [25].

2.3.6 Network density (D)

Density is defined as the ratio of existing edges to the total number of possible edges. It serves as a macro-level proxy for overall economic interdependence. Sharp increases in density are characteristic of systemic crises, whereas post-crisis declines indicate a return to a more differentiated structural configuration [25].

2.3.7 Node centrality

Centrality measures, including degree and betweenness centrality, identify structurally pivotal indicators. High-centrality nodes function as critical transmission channels for economic shocks, implying that fluctuations in these indicators exert a disproportionate systemic impact. These metrics are employed to identify systemically important sectors for policy monitoring and institutional risk assessment [26–28].

3 Results

3.1 Global structure of relationships

Spearman correlation matrices for the entire 17-year period revealed a stable cluster structure in the Russian economy (Fig. 3). Visualization of these matrices shows a clear division of indicators into groups within which the relationships are particularly strong.

The first cluster comprises indicators of the real sector. Indices of industrial production, manufacturing, construction, trade, and services demonstrate high mutual correlation, reflecting the synchronicity of business activity across various sectors. Interestingly, mining exhibits a somewhat lower degree of integration within this cluster, indicating the relative independence of the raw materials sector from overall economic dynamics. The second cluster is formed around financial markets. The RTS and Moscow Exchange stock indices are inversely linked to the ruble-dollar exchange rate, reflecting a pattern typical for emerging markets. Federal government bond yields form a subgroup within the financial cluster, demonstrating a link to the Bank of Russia's key rate.

The third cluster includes global prices for various grades of oil, which are almost perfectly correlated with each other but show a variable relationship with Russian macroeconomic indicators. Leading indicators and business climate indicators form a separate group, which also demonstrates correlations with the real sector and financial markets. This is logical, as business expectations are influenced by both current production activity and signals from financial markets.

3.2 Dynamics of network metrics and identification of crisis periods

The most compelling results were obtained by analyzing the temporal evolution of network characteristics (Fig. 4). Graphs of global network metrics demonstrate distinct patterns corresponding to four crisis periods in the Russian economy.

The global financial crisis of 2008–2010 is characterized by a sharp increase in network density and average node strength. This phenomenon, known as stress-induced synchronization, reflects the fact that during crises,

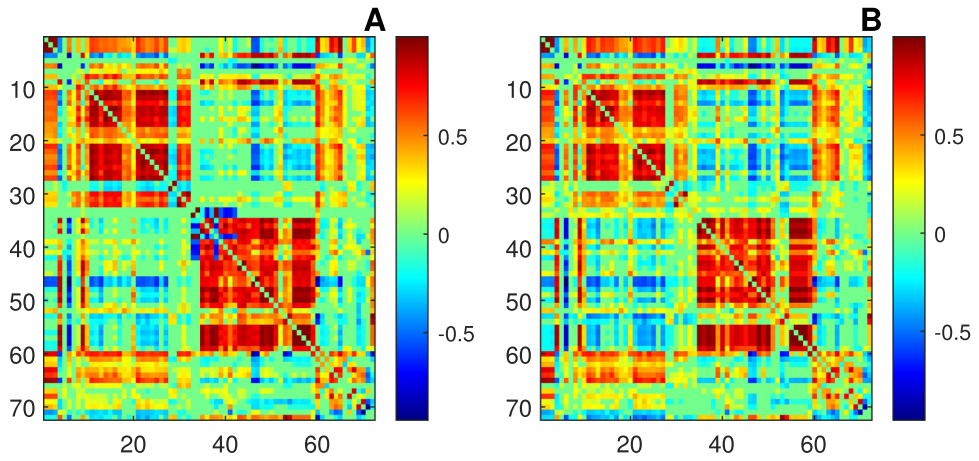


Fig. 3 Global correlation structure of macroeconomic indicators for the period 2008–2025. The left panel shows Pearson correlations, the right panel shows Spearman correlations. The color scale from blue (negative correlation) to red (positive correlation) reflects the strength of the relationship between indicators. A block structure is clearly visible, indicating the existence of stable clusters of inter-related indicators

most economic indicators begin to move in concert, usually in a negative direction. The clustering coefficient also increases, indicating the formation of dense clusters of interconnected indicators [29].

The 2014–2015 currency crisis exhibits a similar, but more pronounced, pattern. The acute phase coincides with peaks in average node strength, indicating that virtually all sectors of the economy were caught in turbulence. Notably, after the acute phase ended in mid-2015, a gradual decline in connection density was observed, reflecting the economy's adaptation to new conditions and the onset of recovery [30].

The 2020–2021 pandemic crisis has a unique profile. The initial phase is characterized by an extreme surge in correlations, driven by a sudden, all-encompassing shock that affected all sectors simultaneously [31].

The period leading up to 2022 and subsequent dynamics reveal an interesting picture. The initial phase is characterized by increasing synchronization of indicators, but then a relatively rapid stabilization occurs at a new level. This may indicate a structural restructuring of the economy and the formation of a new configuration of intersectoral relationships.

Two further global metrics in Fig. 4 reinforce this picture and substantiate the claims made in the Abstract. First, network modularity (Q) drops in synchrony with each of the four crisis episodes, indicating breakdown of sectoral autonomy as previously segmented communities merge into a single co-moving aggregate; this is the network counterpart of the well-known empirical observation that "everything moves together" under stress. Second, the average shortest-path length contracts during the same windows, consistent with accelerated propagation of shocks across the system. Notably, Pearson- and Spearman-based networks (red and blue curves in Fig. 4) track each other closely across all eight metrics throughout the 17-year sample, demonstrating that the reported pattern of stress-induced synchronization, modularity breakdown, and path-length contraction is robust to the choice of correlation measure and not an artefact of any particular monotonicity assumption.

3.3 The special role of node degrees and clustering coefficients

Table 2 reports the top-10 indicators by two complementary centrality measures averaged separately over calm and crisis windows. The rankings provide concrete empirical support for the systemic roles claimed in the abstract.

By degree, monetary aggregates (M2b, M2, M2Xb), business climate indicators (IBC manuf, IBC manuf invest, IBC industry, IBC constr, IBC_all), the RTS stock index, and manufacturing production (Process1) dominate. All these indicators exhibit a marked increase in degree during crises (e.g., M2b from 70.1 to 79.4, IBC manuf from 67.2 to 78.4), reflecting the widespread synchronization of real, financial, and expectation-driven variables under stress. Notably, the ruble exchange rate (RUBUSD) does not appear in the top-10 degree list, indicating that while it is highly connected (its degree is still above average), it is not among the absolute most connected nodes (Fig. 5).

By betweenness, a different set emerges. EX (goods exports), Food1 (public catering turnover), RUBUSD, Build1 (construction), RU3m (short-term OFZ yield), IBC agro (agriculture expectations), RU10Y (long-term OFZ yield), IM (goods imports), and CAB (current account balance) occupy the top ranks. Betweenness measures how often a node lies on the shortest paths between other pairs, its role as a broker or channel for shock transmission. The high betweenness of EX, IM, CAB, and RUBUSD confirms that external sector variables and the exchange rate are critical conduits through which global and domestic disturbances propagate across the economy. The presence

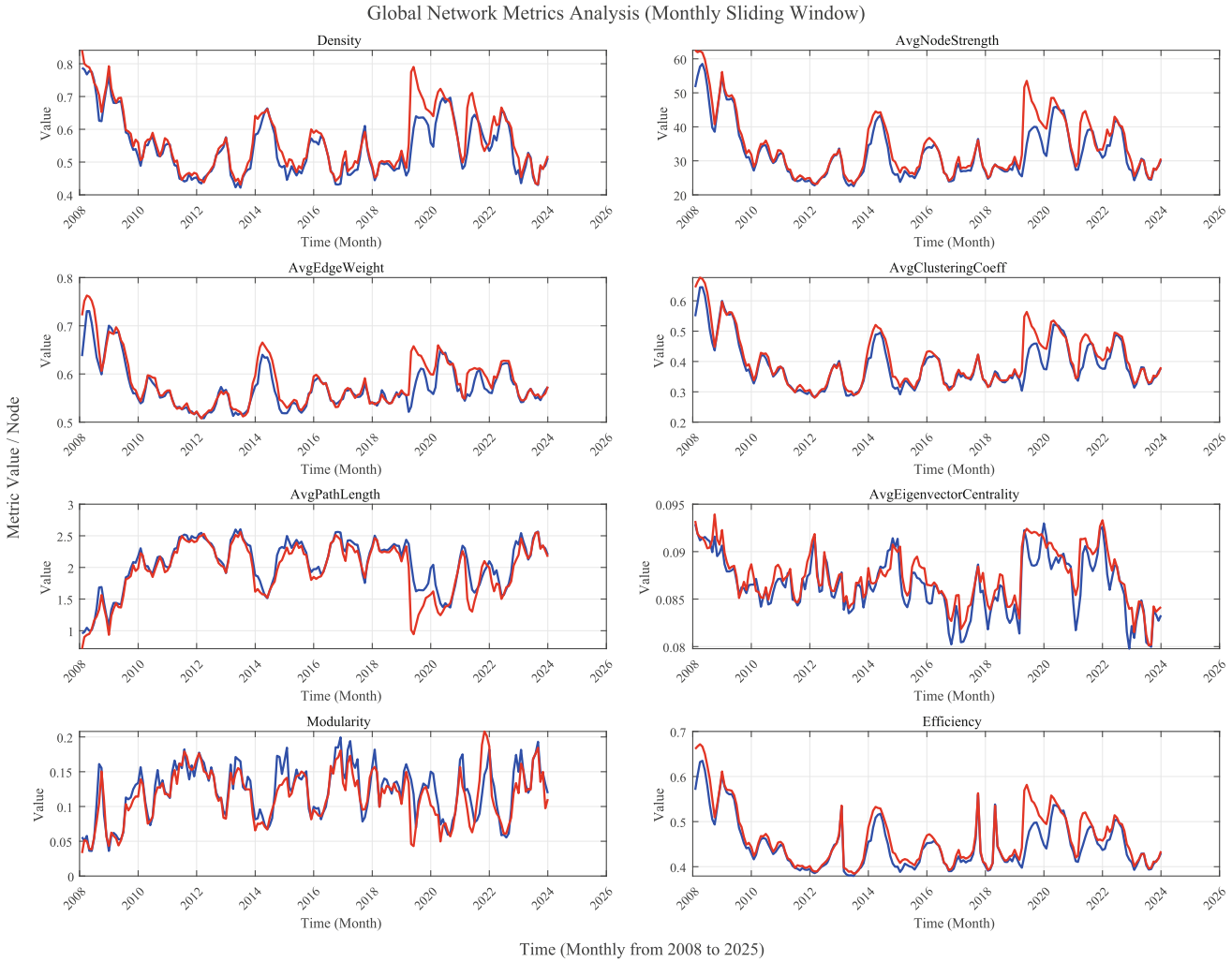


Fig. 4 Dynamics of global network characteristics over a sliding annual window. The top panel shows network density and average node strength, the second panel shows average edge weight and average clustering coefficient, the third panel shows average path length and average eigenvector centrality, and the bottom panel shows network modularity and efficiency. Blue curves correspond to Spearman correlations, red curves to Pearson correlations. The close agreement between Pearson and Spearman trajectories across all eight metrics demonstrates the robustness of the network dynamics to the choice of correlation measure. A systematic increase in edge density and clustering coefficient is evident during periods of crisis

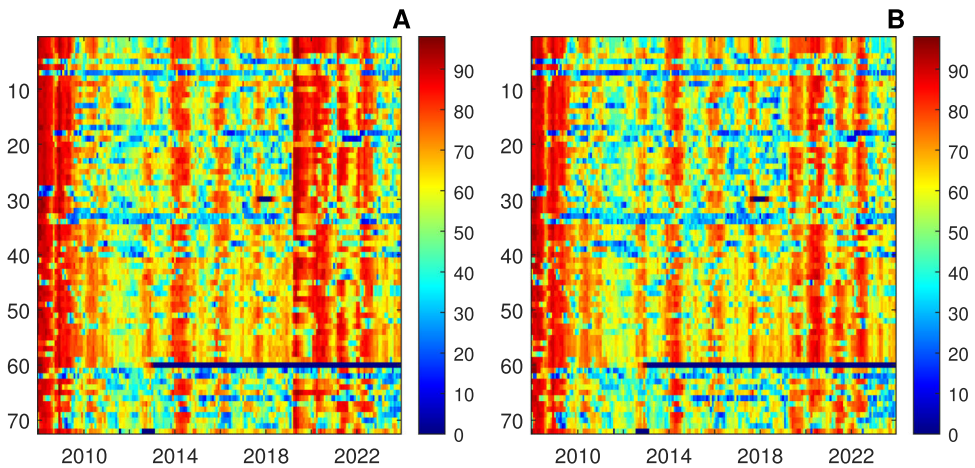


Fig. 5 Node degree dynamics (left—Pearson, right—Spearman). The color map shows the number of significant connections for each indicator at each point in time. Warmer colors correspond to a greater number of connections. Vertical bands of increased connectivity during periods of crisis are clearly visible and outlined in the left picture

Table 2 Top-10 indicators by degree and betweenness centrality, averaged separately over calm and crisis windows

Indicator	Degree_calm	Degree_crisis	Indicator	Betweenness_calm	Betweenness_crisis
M2b	70.11	79.44	EX	68.225	98.0625
IBC manuf	67.19	78.41	Food1	61.475	86.8125
IBC manuf invest	65.19	77.91	IBC manuf	60.575	82.4375
M2	67.51	77.31	RUBUSD	81.4125	76.3125
IBC industry	61.36	76.78	Build1	89.45	74.25
IBC constr	63.49	76.38	RU3m	47.4	73.125
RTS	66.47	75.53	IBC agro	41.7375	73.0625
M2Xb	67.96	75.5	RU10Y	64.05	67.6875
IBC_all	66.25	75.31	IM	79.575	65.875
Process1	67.65	74.88	CAB	61.85	64.9375

of Food1 (catering) and Build1 (construction) suggests that even real sector sub-components can act as structural bridges, presumably because they respond to both household income shocks and supply-chain disruptions.

The heat map of node degrees over time is one of the most informative results of this study. It clearly demonstrates that node degree possesses exceptional sensitivity to crisis phenomena.

A node's degree indicates how many significant correlations a given indicator has with other indicators in the network. During stable periods, various indicators exhibit specific correlation patterns reflecting the structural characteristics of the economy. However, during crises, a dramatic change occurs: almost all nodes simultaneously increase their degree, turning red on the heat map and visually creating distinct vertical bands that precisely coincide with crisis periods.

This effect has a profound economic explanation. Under normal conditions, various sectors can move relatively independently. Industry can grow, while agriculture declines, and financial markets can show optimism amid stagnation in the real sector. During systemic crises, however, this independence vanishes. All sectors are drawn into a common vortex, and indicators begin to move in sync.

Local clustering coefficients complement this picture. The clustering coefficient measures the degree to which a given node's neighbors are also interconnected. A high clustering coefficient means that the metrics associated with a given indicator are closely related to one another, forming a dense local structure.

Analysis of the temporal dynamics of local clustering coefficients shows that they also increase during crises, but with a specific pattern. The most significant increases are observed for financial market indicators and exchange rates at the onset of crises, reflecting the fact that financial indicators are usually the first to react to impending turbulence. Real sector indicators show an increase in clustering with a slight lag, corresponding to the time required for shocks to be transmitted from the financial sector to production activity.

A hypothesis to be tested concerns the behavior of leading indicators, such as PMIs and business climate indicators. Their clustering coefficients should potentially begin to increase earlier than most other indicators, confirming their ability to detect changes in the economic environment at early stages. This opens the possibility of using the dynamics of network metrics for these indicators as an early warning signal of impending crises.

Because C_i measures the density of closed triangles around each node, its growth in crisis windows is the most direct empirical signature of higher-order (triadic) coordination among macroeconomic indicators: it captures the formation of locally complete 2-simplices that cannot be inferred from pairwise degree alone. The fact that this higher-order signal rises sharply and broadly during all four crisis episodes—across both Pearson- and Spearman-thresholded networks—supports the use of C_i as a key building block of an early-warning system for self-organized macroeconomic synchronization.

4 Discussion

4.1 Crisis early warning system

The most immediate application of this research is the creation of a systemic risk monitoring system based on network metrics. Since node degrees and clustering coefficients exhibit consistent changes in the lead-up to and during crises, they can be incorporated into a composite risk index. Such an index would track not only traditional volatility or macroeconomic imbalance indicators but also subtle changes in the structure of relationships between economic indicators.

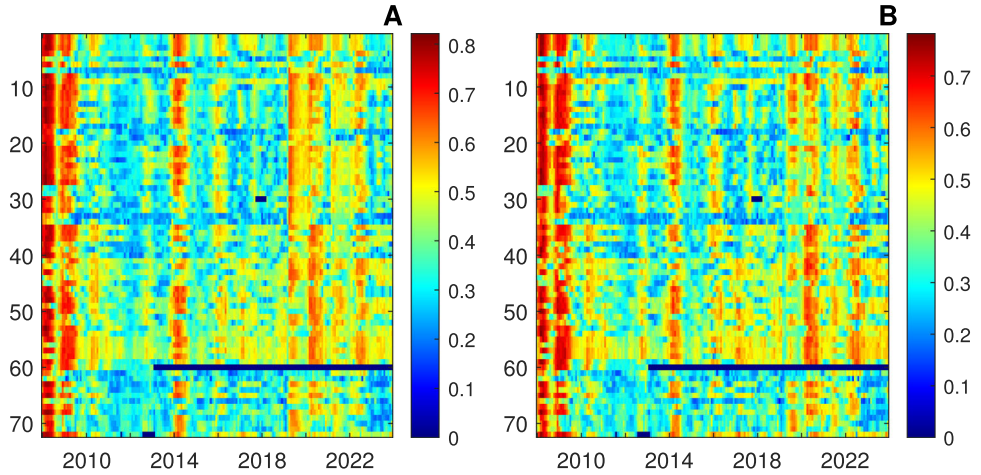


Fig. 6 Dynamics of the node clustering coefficient (network thresholded on Pearson correlations on the left, on Spearman correlations on the right). The color map shows the local clustering coefficient C_i for each indicator over time. Warmer colors correspond to higher local clustering, i.e., a denser triangular (2-simplex) neighbourhood around the indicator. Vertical bands of increased clustering during periods of crisis are clearly visible

Crucially, changes in the network structure often outpace the deterioration of the indicators themselves. The economy may begin to enter a state of heightened synchronization even before the main macroeconomic indicators show clear signs of distress. Monitoring this process would provide development institutions with additional lead time to prepare anti-crisis measures and protect investment project portfolios.

4.2 Assessing the systemic importance of sectors and projects

Analyzing node centrality in a functional network allows for the identification of sectors and activities that play a key role in the economic system. Indicators with high centrality—such as degree centrality (number of connections) or betweenness centrality (control over information flows)—represent critical nodes through which the main channels of economic impulse transmission pass [26, 27].

This enables more precise prioritization of investment activities. Projects in sectors central to the network, like energy or manufacturing in input–output models, exhibit stronger multiplier effects on the entire economy, amplifying GDP impacts by 1.5–2 times compared to peripheral sectors [32]. Conversely, such sectors are more vulnerable to systemic risks, such as supply chain disruptions, which must be factored into project risk assessments using metrics like eigenvector centrality to quantify indirect influences. The dynamic nature of the analysis, via time-varying networks, allows tracking how the role of various sectors changes over time. For instance, sectors like agriculture that were previously peripheral can shift to the network core due to import substitution policies amid sanctions. Early detection of such shifts, through rolling window estimations, facilitates resource reallocation to the most promising areas, enhancing return on investment for development banks.

4.3 Analysis of transmission channels and chain effects

The structure of a functional network reveals the pathways through which shocks propagate across the economic system. Knowledge of the connection topology—via directed edges representing correlation strengths—enables prediction of affected sectors and estimation of spillover effects, such as second-round impacts from input–output linkages [33].

This has direct implications for assessing investment project risks. Traditional analysis considers risks specific to a particular project or industry, like commodity price volatility. We hypothesize that the network approach adds a dimension of interconnected risks, modeling cascades, where a shock in one node triggers failures in densely connected clusters. For example, a disruption in logistics (high degree centrality) can propagate to manufacturing and retail, materially elevating default probabilities in linked sectors [34]. A project in a sector that appears resilient in isolation, such as domestic tech, may prove vulnerable due to strong inbound links from sanctioned imports.

4.4 Scenario planning and stress testing

Understanding how the structure of economic relationships changes across different types of crises allows for the development of more realistic scenarios for stress testing. Instead of simply assuming a deterioration in individual indicators, we can model the reconfiguration of the entire network—e.g., increased modularity or centrality shifts—characteristic of a particular shock type, using historical crisis data for calibration [35].

For example, a currency crisis often exhibits a network profile of rapid financial-real sector synchronization, followed by fragmentation, as seen in the 2014–2015 Russian rouble crisis [36]. In contrast, a demand-drop crisis, like the 2008–2009 global recession, shows gradual spillover from consumer goods to upstream industries. A financial crisis is characterized by initial synchronization of financial indicators (e.g., rising correlations in banking metrics) followed by spillover into the real sector, while a real sector crisis may follow the reverse sequence, starting with production halts. Incorporating these patterns via agent-based or vector autoregression network models makes scenario analysis more detailed and practically useful, improving forecast accuracy for investment portfolios [37]

4.5 Monitoring the structural transformation of the economy

If the Russian economy is indeed undergoing structural changes in response to sanctions and import substitution pressures, functional network analysis may offer a framework for observing such transformations in near real-time. The network approach cannot directly measure structural change, but changes in community composition and node centrality, such as the emergence of new clusters involving domestic machinery indicators, would be consistent with a reconfiguration of intersectoral linkages. These patterns are suggestive and warrant further investigation using directed causal methods. [38].

The emergence of new connection clusters (e.g., in domestic machinery substituting for imports), changes in centrality of sectors, such as chemicals or IT, and formation of alternative interaction chains replacing broken external ties—all become visible through metrics like community detection algorithms (e.g., Louvain method [39]). This enables development institutions to assess the effectiveness of structural adjustment support measures—e.g., tracking if import substitution boosts network resilience—and promptly adjust strategies, such as redirecting funds to rising centrality nodes.

4.6 Directions for further research

The first priority is a detailed decomposition of crisis periods into phases. For each of the four crises, it is necessary to identify the stages of increasing tension, acute phase, stabilization, and recovery. Based on network metrics, regression models can be constructed to quantitatively describe the characteristics of each phase and establish formal criteria for identifying the current stage of the crisis cycle.

The second direction involves using community detection methods to identify stable clusters of indicators and analyze their evolution. Louvain modularity algorithms or Infomap will automatically identify groups of closely related indicators and track how their composition changes over time [40]. Of particular interest is whether new clusters emerge as a result of economic restructuring after 2022.

The third approach involves moving from correlation analysis to causal analysis. Applying the concept of time lags between indicators will allow us to construct directed graphs, where edges indicate not just a relationship but the direction of influence, taking time lags into account. This will provide an understanding of which indicators are drivers of change and which follow with a delay.

The fourth area concerns the integration of microdata on enterprises and projects. Linking the dynamics of macroeconomic network metrics to the performance of specific enterprises or the effectiveness of investment projects will create a bridge between macro- and micro-analysis. This integration will allow the state of the macroeconomic network to be used as a factor in project evaluation models.

The fifth area involves expanding the methodological toolkit. In addition to classic correlation measures, machine learning methods are promising for identifying nonlinear and conditional relationships between indicators. Neural networks can detect complex interaction patterns not captured by traditional statistical methods.

Sixth, higher-order interactions and hypergraph representations. The functional network framework developed in this work relies on pairwise correlations, which capture dyadic relationships between macroeconomic indicators. However, economic systems often exhibit collective effects that cannot be reduced to pairs—for instance, simultaneous co-movement of three or more indicators may emerge during a crisis without any single pair showing exceptionally high correlation. Such higher-order interaction is a genuine multi-node phenomenon [41, 42]. To address this, future research should extend the present graph-based description to hypergraphs or simplicial complexes, where hyperedges can connect an arbitrary number of nodes. Recent methodological advances in functional neuroimaging have demonstrated that higher-order (triadic and beyond) interactions reveal emergent dynamics inaccessible to conventional pairwise analysis [43]. Translating these tools to macroeconomics would allow us to quantify true multi-variate co-movement, for example, by computing partial correlations conditioned on a third

indicator, or by constructing simplicial complexes from correlation hypergraphs with a significance threshold on the mutual information of triples. The local clustering coefficient C_i used in this study is the simplest higher-order measure (it counts closed 2-simplices, i.e., triangles). A systematic comparison between C_i and full hypergraph statistics—such as hyperedge degree distribution, hypergraph modularity, and topological invariants of the simplicial complex—should be undertaken. This would bridge the gap between dyadic stress-induced synchronization and true multi-node collective regimes, potentially yielding earlier, more specific early-warning signals and a deeper understanding of how macroeconomic self-organization proceeds beyond pairwise interactions.

5 Conclusion

The presented methodology for constructing functional networks of macroeconomic indicators represents an innovative tool for the systemic analysis of an economy. Its uniqueness lies in its ability to simultaneously encompass multiple dimensions of the economic system and track the dynamic evolution of its inter-relational structure.

The results obtained demonstrate the high sensitivity of network metrics to crisis phenomena. Node degrees and clustering coefficients show distinct changes during periods of turbulence, opening the possibility of using them for the early warning of systemic risks. The visual clarity of the heat maps makes the analysis results easily interpretable not only by network analysis specialists but also by a wide range of economists and policymakers.

Conceptually, the dynamics we report position the macroeconomic system within the framework of self-organization and higher-order interactions in complex networks. The simultaneous collapse of modularity, contraction of average path length, and growth of the local clustering coefficient describe the spontaneous emergence of a globally coherent, low-dimensional regime under stress; and the clustering coefficient itself—by counting closed triangles around each indicator—constitutes the most direct, computationally light measure of triadic (2-simplex) interaction in the system. The robustness of this picture across Pearson- and Spearman-based networks lends additional support to the proposed interpretation. A principal limitation of this approach is that correlation-based functional networks capture statistical synchrony rather than causal direction, causal inference remains a priority for future work.

We see significant potential for the further development and practical application of this methodology.

Acknowledgements We thank Dr. Andrei Klepach for his interest in our work and for the fruitful discussions.

Funding The article was prepared as part of research project No. FSSW-2026-0008 “Development of fundamental principles for constructing digital twins of infrastructure systems in the data economy” using funds from a subsidy from the federal budget within the framework of the state assignment of the Ministry of Education and Science of Russia.

Data Availability The data presented in this study are available on request from the corresponding author.

Appendix 1

The following economic time series were selected for the analysis, ranging from February 2008 to February 2025:

1. Brent crude oil—USD/ bbl—average for the period; code—Brent [44].
2. Dubai crude oil—USD/ bbl—average for the period; code—Dubai [44].
3. WTI crude oil—USD/ bbl—code—WTI [44].
4. The dollar to ruble exchange rate is rub./dollar—average for the period; code—RUBUSD [45].
5. Index of the real effective exchange rate of the ruble to foreign currencies—% m/m; code—RUBOTH [45].
6. Euro to dollar exchange rate—USD/EUR – forex, monthly average; code—USDEUR.
7. GDP—% m/m—in real terms, seasonally adjusted; code—GDP-1 [46].
8. GDP—% y/y —in real terms; code—GDP-12 [46].
9. GDP index—Jan 2008 = 100—calculation; code—GDP_i [46].
10. News Index - Points (Bank of Russia—published on the 4th of each month and describes the situation for the previous month; code—news_index [47].
11. Business climate indicator IBC (expectations) for industry—data—month of filling out questionnaires, the survey of enterprises is carried out in the first 10 days of the month, s.s.; code—IBC_all [48].
12. Business climate indicator IBC (expectations) for the economy; code—IBC industry [48].
13. Business climate indicator IBC (expectations) for production; code—IBC mining [48]
14. Business climate indicator IBC (expectations) for manufacturing industries; code—IBC manuf [48]

15. Business climate indicator IBC (expectations) for consumer-oriented manufacturing industries; code—IBC manuf potr [48].
16. Business climate indicator IBC (expectations) for manufacturing investment industries; code—IBC manuf invest [48].
17. Business climate indicator IBC (expectations) for intermediate-purpose manufacturing industries; code—IBC manuf prom [48].
18. Business climate indicator IBC (expectations) for the provision of electricity, gas and steam; code—IBC utilities [48].
19. Business climate indicator IBC (expectations) for water supply; code—IBC water [48].
20. Indicator IBC (expectations) for agriculture; code—IBC agro [48].
21. Business climate indicator IBC (expectations) for construction; code—IBC constr [48].
22. Business climate indicator IBC (expectations) for trade; code—IBC trade [48].
23. Business climate indicator IBC (expectations) for auto trade; code—IBC trade auto [48].
24. Business climate indicator IBC (expectations) for wholesale trade; code—IBC trade opt [48].
25. Business climate indicator IBC (expectations) for retail trade; code—IBC trade rozn [48].
26. Business climate indicator IBC (expectations) for transportation and storage; code—IBC storage [48].
27. Business climate indicator IBC (expectations) for services; code—IBC serv [48].
28. Consumer prices –% m/m—seasonally adjusted, published approximately in the middle of the month; code—CPI m sa [49].
29. Consumer prices for basic goods and services—% m/m—seasonally adjusted, published approximately in the middle of the month; code—CPI core m sa [49].
30. Purchasing Managers' Index Composite PMI - Points; code—PMI comp [50].
31. Manufacturing Purchasing Managers' Index (PMI) - Points ; code—PMI manuf [50].
32. Services PMI Purchasing Managers' Index - Points; code—PMI serv [50].
33. Composite Leading Index—points; code - CLI [51].
34. Agricultural production—% y/y (Rosstat)—dynamic series for AI_1.xlsx; code—Agro1.
35. Industrial production – % y/y (Rosstat)—dynamic series for AI_1.xlsx; code—Industry1.
36. Mining and quarrying – % y/y (Rosstat)—dynamic series for AI_1.xlsx; code—Natural1.
37. Manufacturing—% y/y (Rosstat)—dynamic series for AI_1.xlsx; code—Process1.
38. Production and distribution of electricity, gas, and water—% y/y (Rosstat)—dynamic series for II_1.xlsx; code—Electro1.
39. Construction—% y/y (Rosstat) – dynamic series for AI_1.xlsx; code—Build1.
40. Cargo turnover—% y/y (Rosstat) – dynamic series for II_1.xlsx; code—Cargo1.
41. Retail trade—% y/y (Rosstat)—dynamic series for AI_1.xlsx; code—Trade1.
42. Wholesale trade—% y/y (Rosstat)—dynamic series for AI_1.xlsx; code—OptTrade1.
43. Paid services—% y/y (Rosstat)—dynamic series for AI_1.xlsx; code—Service1.
44. Public catering—% y/y (Rosstat)—dynamic series for AI_1.xlsx; code—Food1.
45. Gold—$/ounce (price)—calculation; code—Gold.
46. Dollar index to developed country currencies—Index: 2006 Jan 100; code—DollarNAFE.
47. Dollar index against major currencies—Index: 1973 May 100; code—NMDI.
48. DowJones Ind – (index); code—DowJ.
49. S&P500—(index); code—S&P500.
50. Nasdaq—(index); code—Nasdaq.
51. UST3m—% (UST)—avg . month; code—UST3m.
52. UST10Y—% (UST)—avg . month; code—UST10Y.
53. RU3m—% (OFZ)—average month; code—RU3m.
54. RU10Y—% (OFZ)—average month; code—RU10Y.
55. M2—(billion rubles)—NSA; code—M2.
56. M2X—(billion rubles)—NSA; code—M2X.
57. M2 —(billion rubles)—SA ; code—M2b.
58. M2X— (billion rubles)—SA; code—M2Xb.
59. RTS—dollar—by trading days; code—RTS.
60. Moscow Exchange Index—ruble—by trading days; code—MOEX.
61. FI_IN—(PB, financial account, growth of liabilities to non-residents, billion dollars); code—FI_IN.
62. FI_OUT—(PB, financial account, growth of foreign assets, billion dollars); code—FI_OUT.
63. EX—(export of goods, million dollars); code—EX.
64. IM—(import of goods, million dollars); code—IM.
65. URALS—(price of Russian oil , USD/ bbl .); code—URALS.
66. Res—(growth of international reserves (operations of the Ministry of Finance and the Central Bank), billion dollars); code—Res.
67. CAB—(current account balance, billion dollars); code—CAB.

68. TB—(trade balance, million dollars); code—TB.
69. EXS—(export of services, billion dollars); code—EXS.
70. IMS—(import of services, billion dollars); code—IMS.
71. BS—(balance of services, billion dollars); code—BS.
72. key_rate—Key rate; code—Key_rate.

References

1. A. Taylor, Two-way street: speech by Alan Taylor—bankofengland.co.uk (2026). https://www.bankofengland.co.uk/speech/2026/april/alan-taylor-at-a-joint-conference-at-the-banque-de-france
2. J.S. Rojas Rincón, J.C. Acosta-Prado, J.E. Castellanos Narciso, A bibliometric analysis on network-based systemic risk. Risks **13**(11), 210 (2025)
3. V. Pacelli, Systemic risk and complex networks in modern financial systems, in *Systemic Risk and Complex Networks in Modern Financial Systems* (Springer, 2024), pp. 3–19
4. D.J. Lurie, D. Kessler, D. Bassett, R.F. Betzel, M. Breakspear, S. Keilholz, On the nature of resting fmri and time-varying functional connectivity. Advance online publication. **24**, 10–31234 (2018)
5. Q. Zhang, W. Wang, J. She, Z. Ma, Understanding bus network delay propagation: integration of causal inference and complex network theory. J. Transp. Geogr. **123**, 104098 (2025)
6. Q. Fang, X. Qiao, Z. Wang, Time series gaussian chain graph models (2026). arXiv:2604.07018
7. S. Oldham, B. Fulcher, L. Parkes, A. Arnatkevicie, C. Suo, A. Fornito, Consistency and differences between centrality measures across distinct classes of networks. PLoS ONE **14**(7), e0220061 (2019)
8. C.E. Mattsson, F.W. Takes, E.M. Heemskerk, C. Diks, G. Buiten, A. Faber et al., Functional structure in production networks. Front. Big Data **4**, 666712 (2021)
9. R.P. Rohr, R.E. Naisbit, C. Mazza, L.F. Bersier, Matching–centrality decomposition and the forecasting of new links in networks. Proc. R. Soc. B Biol. Sci. **283**(1824) (2016)
10. D. Liu, Z. Yang, K. Qin, K. Li, Spatial-temporal analysis of the international trade network. Geo-Spatial Inf. Sci. **28**(5), 2567–2595 (2025)
11. G. Lagarda, Macroeconomics and networks. Foro de Investigadores de Bancos Centrales del Consejo Monetario Centroamericano (2014)
12. K.M. Lee, J.S. Yang, G. Kim, J. Lee, K.I. Goh, K. Im, Impact of the topology of global macroeconomic network on the spreading of economic crises. PLoS ONE **6**(3), e18443 (2011)
13. M. Barigozzi, G. Cavaliere, G. Moramarco, Factor network autoregressions. J. Bus. Econ. Stat. **43**(4), 1105–1118 (2025)
14. S. Bekiros, A. Paccagnini, On the predictability of time-varying var and dsge models. Empir. Econ. **45**(1), 635–664 (2013)
15. A. Feto, M. Jayamohan, A. Vilks, Applicability and accomplishments of dsge modeling: a critical review. J. Bus. Cycle Res. **19**(2), 213–239 (2023)
16. A.J. Bishara, J.B. Hittner, Testing the significance of a correlation with nonnormal data: comparison of Pearson, spearman, transformation, and resampling approaches. Psychol. Methods **17**(3), 399 (2012)
17. E. Benedetti, M. Pučić-Baković, T. Keser, N. Gerstner, M. Büyüközkan, T. Štambuk et al., A strategy to incorporate prior knowledge into correlation network cutoff selection. Nat. Commun. **11**(1), 5153 (2020)
18. H. Esmalifalak, A. Moradi-Motlagh, Correlation networks in economics and finance: a review of methodologies and bibliometric analysis. J. Econ. Surv. **39**(3), 1252–1286 (2025)
19. X. Zhang, D. Tang, S. Kong, X. Wang, T. Xu, V. Boamah, The carbon effects of the evolution of node status in the world trade network. Front. Environ. Sci. (2022). https://doi.org/10.3389/fenvs.2022.1037654
20. S. Furuya, K. Yakubo, Generalized strength of weighted scale-free networks. Phys. Rev. E **78**(6), 066104 (2008). https://doi.org/10.1103/physreve.78.066104
21. N. Masuda, M. Sakaki, T. Ezaki, T. Watanabe, Clustering coefficients for correlation networks. Front. Neuroinform. (2018). https://doi.org/10.3389/fninf.2018.00007
22. K.H. Tuhin, A. Nobi, M.J. Sadique, M.I. Rakib, J.W. Lee, Effect of network size on comparing different stock networks. PLoS ONE **18**(12), e0288733 (2023). https://doi.org/10.1371/journal.pone.0288733
23. A. Kharrazi, Y. Yu, A. Jacob, N. Vora, B.D. Fath, Redundancy, diversity, and modularity in network resilience: applications for international trade and implications for public policy. Curr. Res. Environ. Sustain. **2**, 100006 (2020)
24. X. He, R. Zhang, B. Zhu, A generalized modularity for computing community structure in fully signed networks. Complexity **2023**, 1–20 (2023). https://doi.org/10.1155/2023/8767131
25. P. Caraiani, A.M. Dima, C. Păun, T. Stamule, M.V. Vargas, Production networks and resilience: how dense production networks shield economies in financial crisis. PLoS ONE **19**(4), e0302012 (2024)
26. P. Bonacich, Power and centrality: a family of measures. Am. J. Sociol. **92**(5), 1170–1182 (1987)
27. S.P. Borgatti, D.J. Brass, Centrality: concepts and measures. Social networks at work, pp 9–22 (2019)
28. A. Joseph, G. Chen, *Network Centrality and Key Economic Indicators: A Case Study* (Springer International Publishing, 2014), pp. 159–180. https://doi.org/10.1007/978-3-319-09683-4_9

29. L. Rajmil, M.J. Fernandez de Sanmamed, I. Choonara, T. Faresjö, A. Hjern, A.L. Kozyrskyj et al., Impact of the 2008 economic and financial crisis on child health: a systematic review. Int. J. Environ. Res. Public Health **11**(6), 6528–6546 (2014)
30. D.L. Kolia, S. Papadopoulos, The levels of bank capital, risk and efficiency in the eurozone and the us in the aftermath of the financial crisis. Quant. Finance Econ. **4**(1), 66 (2020)
31. M.R. Hossain, F. Akhter, M.M. Sultana, Smes in covid-19 crisis and combating strategies: a systematic literature review (slr) and a case from emerging economy. Oper. Res. Perspect. **9**, 100222 (2022)
32. D. Acemoglu, F.A. Gallego, J.A. Robinson, Institutions, human capital, and development. Annu. Rev. Econ. **6**(1), 875–912 (2014)
33. A.S. Chakrabarti, A. Chakraborti, S. Upmanyu, Macroeconomic and financial networks: review of some recent developments in parametric and non-parametric approaches, in *Game Theory and Networks: New Perspectives and Directions* (2022), pp. 325–362
34. Y. Li, K. Chen, S. Collignon, D. Ivanov, Ripple effect in the supply chain network: forward and backward disruption propagation, network health and firm vulnerability. Eur. J. Oper. Res. **291**(3), 1117–1131 (2021)
35. P. Glasserman, H.P. Young, How likely is contagion in financial networks? J. Bank. Finance **50**, 383–399 (2015)
36. M. Barigozzi, G. Fagiolo, G. Mangioni, Identifying the community structure of the international-trade multi-network. Phys. A **390**(11), 2051–2066 (2011)
37. T. Kashni, S.F. Albeez, G. Manikandan, H. Haritha, P. Chitra, Ml application in predicting financial markets and supporting data driven investments, in *2025 International Conference on Digital Innovations for Sustainable Solutions (ICDISS)*. (IEEE, 2025), pp. 1–6
38. E. Deryugina, A. Leonidov, A. Ponomarenko, S. Radionov, E. Vasilyeva, Network structure of the economy and the propagation of monetary shocks: the case of Russia. Struct. Change Econ. Dyn. **71**, 315–319 (2024)
39. J. Zhang, J. Fei, X. Song, J. Feng, An improved Louvain algorithm for community detection. Math. Probl. Eng. **1**, 1485592 (2021)
40. V.A. Traag, L. Waltman, N.J. Van Eck, From Louvain to Leiden: guaranteeing well-connected communities. Sci. Rep. **9**(1), 5233 (2019)
41. S. Boccaletti, P. De Lellis, C.I. del Genio, K. Alfaro-Bittner, R. Criado, S. Jalan et al., The structure and dynamics of networks with higher order interactions. Phys. Rep. **1018**, 1–64 (2023)
42. F. Battiston, V. Capraro, F. Karimi, S. Lehmann, A.B. Migliano, O. Sadekar, Higher-order interactions shape collective human behaviour. Nat. Hum. Behav. 1–17 (2025)
43. S.A. Kurkin, A.N. Pisarchik, L.A. Mayorova, A.E. Hramov, Evolution of methods for assessing fmri-based functional networks: from classical pairwise connectivity to higher-order interactions. Phys. Rep. **1174**, 1–66 (2026)
44. World Bank Prospects Group, World bank commodities price data (the pink sheet): Monthly historical data (2025). https://thedocs.worldbank.org/en/doc/18675f1d1639c7a34d463f59263ba0a2-0050012025/related/CMO-Historical-Data-Monthly.xlsx. Accessed 15 Apr 2026
45. Central Bank of Russia, Exchange rate data (2023). https://www.cbr.ru/vfs/statistics/credit_statistics/ex_rate_ind/exchange_rate.xlsx. Accessed 15 Apr 2026
46. Federal State Statistics Service (Rosstat), National accounts. Gross domestic product (2024). https://rosstat.gov.ru/accounts. Accessed 15 Apr 2025
47. Bank of Russia, News index data (2023). https://www.cbr.ru/Content/Document/File/108631/news_index_new.xlsx. Accessed 15 Apr 2026
48. Bank of Russia, Survey data (2023). https://www.cbr.ru/Content/Document/File/135603/mp_survey_data.xlsx. Accessed 15 Apr 2026
49. Bank of Russia, Indicators (2023). https://www.cbr.ru/Content/Document/File/108632/indicators_cpd.xlsx. Accessed 15 Apr 2026
50. S. Global, Press releases (2023). https://www.pmi.spglobal.com/Public/Release/PressReleases. Accessed 15 Apr 2026
51. Higher School of Economics, Data center (2023). https://dcenter.hse.ru/soi. Accessed 15 Apr 2026

Springer Nature or its licensor (e.g. a society or other partner) holds exclusive rights to this article under a publishing agreement with the author(s) or other rightsholder(s); author self-archiving of the accepted manuscript version of this article is solely governed by the terms of such publishing agreement and applicable law.